Journal of Engineering Physics and Thermophysics, Vol. 74, No. 6, 2001

MODELING OF HEAT AND MASS TRANSFER IN SYSTEMS OF RADIATION-EVAPORATION THERMAL PROTECTION

A. P. Kuryachii

UDC 532.516+536.423.1

Results of theoretical and experimental studies of models of different systems of radiation-evaporation thermal protection are presented; the overall-dimension-weight parameters of these systems and of systems of passive radiation thermal protection are compared.

Introduction. Radiation-evaporation systems of combined thermal protection (CTP), whose operating principle was first suggested in [1], are intended for protection of promising spacecraft-aircraft (aerospace vehicles) against intense heating during flight. In both CTP and passive radiation (e.g., plate) thermal protection, the main portion of the heat flux coming to an object is reflected to the environment by radiation from the outer surface of a heat insulation or a special heatproof screen heated to a high temperature. Unlike a passive system, a portion of the heat flux passing through the heat insulation is spent mostly on phase transformations (melting, evaporation, or sublimation) of the cooler lying under the heat insulation.

Being a semiactive thermal protection, CTP combines the advantages of radiation and evaporation systems and has a number of merits over the existing passive (radiation or sublimation) and active (convection or transpiration) systems of thermal protection. As will be shown below, as compared to a passive plate system, a substantial reduction in the thickness of the heat insulation with simultaneous considerable decrease in the total weight of the system is possible in combined thermal protection.

In contrast to active transpiration or convection systems, CTP has no additional elements such as tanks with a coolant and pipelines and pumps for its supply to the working zone. Another advantage of CTP is self-regulation, since the flow rate of the coolant is determined by the heat flux coming to its carrier. These factors guarantee the reliability and stability of CTP operation. The possibility of regulating the temperature of the structure protected by controlling the pressure of the vapor in the evaporation cavity is an additional merit of CTP.

The considered systems are promising and require both theoretical and experimental study. The development of mathematical models of very complex processes of heat and mass transfer is important in both designing these systems and conducting the corresponding experiments. Theoretical simulation must allow one to estimate the effect of the main parameters of CTPs on the performance characteristics of these processes and, on this basis, to optimize the necessary tests [2]. A combined radiation-evaporation method can be realized in different systems which differ in both structural intricacy and efficiency [1–4]. In the present work, we are dealing with three different combined systems of thermal protection in comparison to passive radiation thermal protection.

Theoretical and Experimental Modeling of CTP1. The system considered below can be used for thermal protection of a structure with a free internal cavity. The experimental model tested is a cylindrical structure with a diameter of 210 mm, a height of 25 mm, and a 1.5-mm-thick flat base. The model has a

N. E. Zhukovskii Central Aerohydrodynamics Institute, Zhukovskii, Moscow Region, Russia; email: sasha@kura.aerocentr.msk.su. Translated from Inzhenerno-Fizicheskii Zhurnal, Vol. 74, No. 6, pp. 43–52, November–December, 2001. Original article submitted October 30, 2000.

 1062-0125/01/7406-1412$25.00

1-mm-thick removable cover at the center of which there is a drainage hole with a variable diameter. The model is made of aluminum alloy.

The layer of material of thickness h_d = 4 mm, which damps thermal stresses, is pasted onto the outer surface of the model base, and a layer of heat insulation made of superthin quartz fiber is pasted onto the material layer. The plate thickness h_i is one of the main variable parameters of the systems modeled. The structure described is a model of a system of radiation thermal protection (RTP). Apart from the elements mentioned, the CTP1 model has a capillary-porous layer pasted onto the inner surface of the base and used as the coolant (water) carrier.

The technique and the results of experimental investigations of the given RTP and CTP1 models are described in [5] in detail. During the tests, the temperature of the outer surface of the plate T_e and the air pressure in the vacuum chamber were reproduced in accordance with their specified dependences on time. These dependences [5] model a typical thermal effect on a reusable orbital spacecraft in its flight in the atmosphere for about 60 min with a maximum temperature of heat insulation equal to 1370 K. The main purpose of the tests was determination of the minimum weight of both systems of thermal protection provided that the maximum temperature of the model base does not exceed 433 K during the specified external thermal effect. We note that the main drawback of the experimental technique of [5] is the absence of a guard heater near the cover of the model which resulted in the presence of uncontrolled heat exchange with the environment.

The considered systems are modeled numerically in a one-dimensional approximation. The coordinate axis x is introduced along the normal to the model base with the origin on the outer surface of the plate. It is assumed that the heat transfer in both the plate and the damping layer can be described with the effective coefficient of thermal conductivity λ, which includes all three components of heat transfer: thermal conductivity of a solid matrix, radiation in a fiber medium, and thermal conductivity of a gas at a specified external pressure. Radiative heat transfer in semitransparent heat-shield materials can satisfactorily be calculated in the Rosseland approximation. The thermal conductivity of a gas can be approximated with account for its dependence on the pressure, the temperature, and the diameter of fibers [6]. In the present consideration, by analogy with [6], the following formulas that have been obtained as a result of numerical interpolation of experimental data are taken for the effective coefficient of thermal conductivity λ_i and the specific heat capacity c_i of a quartz plate:

$$\lambda_i(T) = 1.076\cdot10^{-2} + 6.109\cdot10^{-5}\left(\frac{T}{100}\right)^3 + \lambda_g, \quad \text{W}/(\text{m}\cdot\text{K}), \tag{1}$$

$$\lambda_g = \lambda_a\left[\left(1 + A\frac{\rho_i}{\rho_{i0}}\right)^{-1} + 2\left(\frac{2}{\xi} - 1\right)\frac{l}{b}\right]^{-1}, \quad l = 1.255\frac{\mu_a}{\rho_a\sqrt{R_aT}}, \tag{2}$$

$$\lambda_a = 2.1\cdot10^{-3}\frac{T^{2/3}}{T + 122}, \quad \mu_a = 7.2\cdot10^{-4}\lambda_a;$$

$$c_i(T) = 32.13 + 1.91T - 7.19\cdot10^{-4}T^2, \quad \text{J}/(\text{kg}\cdot\text{K}). \tag{3}$$

Here ρ_i = 140 kg/m^3 is the density of the quartz plate and ρ_{i0} = 2650 kg/m^3 is the density of the material of the plate fibers. The best correlation with the available experimental data was obtained for the following values of the parameters: ξ = 0.9, A = 9.5, and b = 5·10^{-5} m. The dependences of the effective coefficient of thermal conductivity of the plate on the temperature and the external pressure, which are based on Eq. (1),

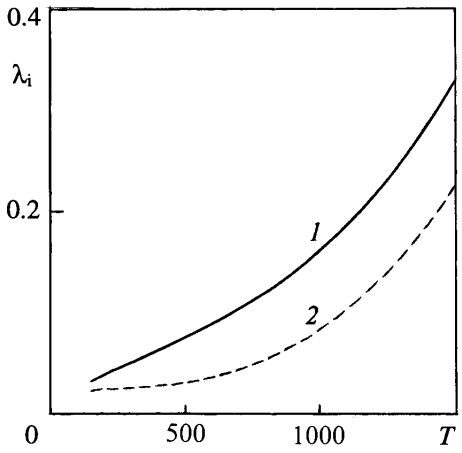

Fig. 1. Temperature dependences of the effective coefficient of thermal conductivity of a quartz plate at atmospheric pressure (1) and in vacuum (2). λ_i, W/(m·K); T, K.

are shown in Fig. 1. The coefficient of thermal conductivity and the specific heat capacity of the damping material are also interpolated by formulas (1) and (3) with different coefficients.

The boundary-value problem of heat transfer in the plate and the damping layer with account for the heat exchange between the base and the cover of the model and the environment has the form

$$\rho_k c_k \frac{\partial T}{\partial t} = \frac{\partial}{\partial x}\left(\lambda_k \frac{\partial T}{\partial x}\right) \quad (k = \text{i, d}) ; \tag{4}$$

$$t = 0 : \; T(x) = T_\text{f} = T_\text{c} = T_\text{a} = T_0 ; \quad x = 0 : \; T = T_\text{e}(t) ; \tag{5}$$

$$x = h_\text{i} : \; (T)_\text{i} = (T)_\text{d} , \quad \left(\lambda \frac{\partial T}{\partial x}\right)_\text{i} = \left(\lambda \frac{\partial T}{\partial x}\right)_\text{d} ; \tag{6}$$

$$x = h_\text{i} + h_\text{d} : \; T = T_\text{f} , \quad -\lambda_\text{d} \frac{\partial T}{\partial x} = C_\text{f} \frac{dT_\text{f}}{dt} + \beta_1 (T_\text{f} - T_\text{c}) - \lambda_\text{eff} \left(\frac{\partial T}{\partial x}\right)_\text{c.c} ; \tag{7}$$

$$C_\text{c} \frac{dT_\text{c}}{dt} = \beta_1 (T_\text{f} - T_\text{c}) - \beta_2 (T_\text{c} - T_\text{a}) . \tag{8}$$

Here T_f, T_c, and T_a are the temperatures of the base and the cover of the model and the surrounding air, respectively, C_f and C_c are the total heat capacities of the base with a cylindrical wall and the cover of the model related to unit surface, and β_1 and β_2 are the coefficients of heat exchange between the base and the cover of the model and between the cover and the environment. We note that possible jumps of the temperature in the glue joints and the thermal conductivity of the glue are not taken into account in the boundary conditions (6) and (7). The last term in the second condition (7) is introduced only in numerical modeling of CTP1 and denotes the heat flux coming to the coolant carrier. Equation (8) serves for determination of the temperature of the model cover.

The following procedure is used for determining the unknown coefficients of heat transfer β_1 and β_2. It was found during the tests that the temperatures of the model base, the cover, and the glue joint of the

plate with a damping layer reach their maximum values $T_{\rm f}^{\max}$, $T_{\rm c}^{\max}$, and $T_{\rm d}^{\max}$ almost simultaneously. In this case, we can neglect all the nonstationary terms in both the equation of heat transfer in the damping layer (4) and conditions (7) and (8). Therefore, the heat flux to the model base and the corresponding coefficients of heat transfer for the indicated instant of time can be estimated in the following way:

$$q = \lambda_{\rm d} \frac{T_{\rm d}^{\max} - T_{\rm f}^{\max}}{h_{\rm d}}, \quad \beta_1 = \frac{q}{T_{\rm f}^{\max} - T_{\rm c}^{\max}}, \quad \beta_2 = \frac{q}{T_{\rm c}^{\max} - T_{\rm a}}. \tag{9}$$

Based of the results of testing the RTP model (plate thickness $h_{\rm i}$ = 46 mm) and formulas (9) we calculated values of the coefficients of heat transfer $\beta_1 \cong 25$ W/(m^2·K) and $\beta_2 \cong 5$ W/(m^2·K).

According to the experimental study [5], the minimum mass per unit area and the thickness of the plate of thermal-protection systems corresponding to it, which provide the required maximum temperature of the model base, are 6.21 kg/m^2 and 43.5 mm for RTP and 5.35 kg/m^2 and 22 mm for CTP1. Thus, the decrease in the total weight of CTP1, as compared to RTP, reached in the experiments amounts to about 14%.

In theoretical modeling of CTP1, the processes of heat and mass transfer and phase transformations in a capillary-porous coolant carrier were taken into account on the basis of the approach of [7]. In contrast to a traditional form [7, 8], the system of equations was represented in a divergent form convenient for numerical calculations [9]:

$$\frac{\partial}{\partial t}\left[c_{\rm eff}\,\rho_{\rm c.c} T + r_0 \Pi\,(1-\alpha)\,\rho_{\rm v}\right] = \nabla\left(\lambda_{\rm eff}\nabla T - r_0\, j_{\rm v} - T\sum_i c_{pi}\, j_i\right) \quad (i = \text{liq, v, a}),$$

$$c_{\rm eff} = c_{\rm c.c} + \frac{\Pi}{\rho_{\rm c.c}}\left[c_{\rm liq}\,\rho_{\rm liq}\alpha + (1-\alpha)\,(c_{v\rm v}\,\rho_{\rm v} + c_{v\rm a}\,\rho_{\rm a})\right],$$

$$\Pi\frac{\partial}{\partial t}\left[(1-\alpha)\,\rho_{\rm v} + \alpha\rho_{\rm liq}\right] + \nabla\,(j_{\rm liq} + j_{\rm v}) = 0, \quad \Pi\frac{\partial}{\partial t}\left[(1-\alpha)\,\rho_{\rm a}\right] + \nabla j_{\rm a} = 0,$$

$$j_i = -\,(1-\alpha)\left[K\frac{\rho_i}{\mu_{\rm g}}\nabla p + D_{\rm eff}\,\rho_{\rm g}\,\nabla\left(\frac{\rho_i}{\rho_{\rm g}}\right)\right] \quad (i = \text{v, a}), \quad \rho_{\rm g} = \rho_{\rm a} + \rho_{\rm v}, \tag{10}$$

$$j_{\rm liq} = -\,a_{\rm liq}\Pi\rho_{\rm liq}\nabla\alpha - K\frac{\rho_{\rm liq}}{\mu_{\rm liq}}\nabla p, \quad \nabla \equiv \frac{\partial}{\partial x},$$

$$p = (\rho_{\rm v}R_{\rm v} + \rho_{\rm a}R_{\rm a})\,T, \quad \rho_{\rm v} = \rho_{\rm v.s}\,(T) = \frac{133.4}{R_{\rm v}T}\exp\left(18.681 - \frac{4105}{T-35}\right).$$

Here $c_{\rm eff}(\alpha)$ and $\lambda_{\rm eff}(\alpha)$ are the effective specific heat capacity and the coefficient of thermal conductivity of moist capillary-porous material, α is the volume concentration of the liquid in the pore (moisture content), r_0 is the specific heat of evaporation at 0 K, and $D_{\rm eff}$ is the effective coefficient of diffusion of the vapor in the air that allows for the crookedness of the pores [10].

Equations (10) describe the flow of a vapor-air mixture which is independent of the flow of a liquid. When the moisture content is rather high, the air becomes restrained in the pores of the material. In this case, in consideration of combined flow of the gas and the liquid the velocities of both phases are assumed to be the same. Therefore, the flows of the air and the vapor can be defined as

$$j_{\rm a} = \frac{1-\alpha}{\alpha}\frac{\rho_{\rm a}}{\rho_{\rm liq}} j_{\rm liq}\,,\quad j_{\rm v} = \frac{\rho_{\rm v}}{\rho_{\rm a}} j_{\rm a}\,. \tag{11}$$

Moreover, it is assumed that transition from the state of air restraint to independent flow of the phases occurs with decrease in the moisture content within the range $\alpha_{\rm g} \le \alpha \le \alpha_{\rm liq}$, where $\alpha_{\rm g}$ and $\alpha_{\rm liq}$, which depend on the structure of the capillary-porous material, are assumed to be known. For description of the flow of the phases within the entire range of moisture content, the flows of the air and the vapor are represented as $j_i = f j_i^{(1)} + (1-f)\, j_i^2$ ($i = v, a$), where $j_i^{(1)}$ and $j_i^{(2)}$ are determined by expressions (10) and (11), respectively; the function f is continuous with the first derivative, it changes from 0 to 1 within the range $\alpha_{\rm g} \le \alpha \le \alpha_{\rm liq}$ and is equal to 1 when $\alpha \le \alpha_{\rm g}$ and to 0 when $\alpha \ge \alpha_{\rm liq}$.

The base of the model is assumed to be thermally thin. Then, initial and boundary conditions for the presented system of equations have the form

$$h_{\rm i} + h_{\rm d} \le x \le h_{\rm i} + h_{\rm d} + h_{\rm c.c}\,,\quad t = 0:\ T = T_0\,,\quad \alpha = \alpha_0 < 1\,,\quad \rho_{\rm a} = \frac{p_0 - p_{\rm v.s}(T_0)}{R_{\rm a} T_0}\,,$$

$$x = h_{\rm i} + h_{\rm d}:\ j_{\rm v} + j_{\rm liq} = 0\,,\quad j_{\rm a} = 0\,,$$

$$x = h_{\rm i} + h_{\rm d} + h_{\rm c.c}:\ j_{\rm v} + j_{\rm liq} = \frac{W}{S}\frac{\partial \rho_{\rm v}}{\partial t} + \frac{1}{1+Z}\frac{G}{S} + j_{\rm liq.leak}\,,\quad j_{\rm a} = \frac{W}{S}\frac{\partial \rho_{\rm a}}{\partial t} + \frac{Z}{1+Z}\frac{G}{S}\,,$$

$$-\left(\lambda \frac{\partial T}{\partial x}\right)_{\rm c.c} + T \sum_{i={\rm a,v}} c_{pi} j_i + c_{\rm liq} j_{\rm liq} T + r_0 j_{\rm v} = c_{\rm liq} j_{\rm liq.leak} T + \tag{12}$$

$$+ \frac{W}{S}\frac{\partial}{\partial t}\left[(\rho_{\rm a} c_{v{\rm a}} + \rho_{\rm v} c_{vv})\, T + r_0\, \rho_{\rm v}\right] + \frac{G}{S}\frac{(c_{p{\rm a}} Z + c_{p{\rm v}})\, T + r_0}{1+Z}\,.$$

Here $Z = \rho_{\rm a}/\rho_{\rm v}$, $j_{\rm liq.leak}$ is the flow of the liquid displaced from the coolant carrier, and G is the flow rate of the vapor-air mixture through the drainage hole, which is determined by the formulas of adiabatic outflow of the gas from the cavity [11].

The main features of the numerical solution of the formulated problem (10)–(12) are presented in [2]. The coefficients of heat and mass transfer of the capillary-porous material were estimated by comparison of calculated and experimental data. The corresponding technique is also described in [2]. The system of CTP1 was modeled numerically with the following set of parameters of the capillary-porous material: $a_{\rm liq} = 2.5\cdot10^{-12}$ m^2/sec, $\Pi = 0.8$, $\alpha_1 = 0.85$, $\alpha_2 = 0.95$, $D_{\rm eff} = 2\cdot10^{-5}$ m^2/sec, and $K = 4\cdot10^{-14}$ m^2.

Numerical modeling of both systems revealed the importance of excluding uncontrolled leakage of heat in experiments. For example, the maximum temperature of the model base calculated under adiabatic conditions on the cover, i.e., for the heat-transfer coefficients $\beta_1 = \beta_2 = 0$, exceeds the experimental values for different thicknesses of the plate by 130–110 K for RTP and 150–100 K for CTP1. Calculations made for the above-indicated finite values of these coefficients are in good agreement with experimental data in the case of RTP. However, the maximum temperature calculated for the CTP1 model is still 50–30 K higher than that measured. The latter can be explained by the more intense heat transfer from the cover of the model to the environment due to additional convection caused by the outflow of the vapor from the drainage hole and flow around the model cover. Therefore, the value of the coefficient β_2 must be higher in this case.

General Structure of CTP2 and CTP3. The main difference of the two combined systems, which will be considered in what follows, from CTP1 is the placement of the coolant carrier on the outer side of the structure protected against external heating. It is assumed that it has the shape of a flat plate of thickness

h_w with a density of the material ρ_w and a specific heat capacity c_w. We introduce a Cartesian coordinate system with the x axis perpendicular to the plate and directed toward the external heat flux. A layer of material saturated with the coolant is on the outer surface of the plate. Heat and mass transfer and phase transformations in this layer are not considered in the model suggested, in particular, the temperature gradient in the layer is disregarded. Therefore, the origin of the x axis lies on the outer surface of the coolant carrier which is considered to be the evaporation surface. The y axis lies on this surface. We consider an individual fragment of the system of thermal protection of overall length $2L$ toward the y axis ($-L \le y \le L$).

The inner surface of the layer of porous heat insulation lies at a distance x_1 from the evaporation surface. The thickness of the insulation layer is $h_i = x_2 - x_1$, where x_2 is the coordinate of its outer surface. The external flat screen made of dense heatproof material lies at a distance x_3 from the evaporation surface. The screen serves for protection of the porous heat insulation against heavy aerodynamic loads and is considered to be thermally thin. The screen thickness h_e, the density of the material ρ_e, the specific heat capacity c_e, and the radiating power of the surface ε_e are specified. The outer surface of the screen is subjected to the effect of the nonstationary heat flux $q_e(t)$. Part of this flux ($q_r = \varepsilon_e \sigma T_e^4$) is reflected to the environment. Another formulation of the problem presupposes the assignment of a temperature of the external screen $T_e(t)$.

In the first of the systems considered, a superthin screen is placed on the inner surface of the insulation layer that is directed to the coolant carrier. This screen ensures the impermeability of the insulation layer to gas and a high thermal resistance of the range $0 \le x \le x_1$ for a small value of the radiating power of the screen surface ε_s. The coolant is evaporated to a flat channel of finite length that is formed by this reflecting screen and the evaporation surface. The channel has a symmetry axis at $y = 0$. Both ends of the channel converge, thus ending with slots of width δ. The converging parts of the channel and the slots model a real drainage system. The vapor flows out of this channel to the environment with a pressure $p_e(t)$. This version of thermal protection has the name CTP2. The second version, denoted as CTP3, does not have the internal reflecting screen. The coolant vapor flows through the layer of porous heat insulation to the channel between this layer and the external heatproof screen. Then the vapor flows out through the drainage holes.

Modeling of CTP2. In the general case, one can use a packet of different heat-insulation materials as an insulation layer in CTP2. However, to compare this system to a passive radiation one we will consider the quartz plate described in the previous sections. It is assumed that variation in the temperature of the external screen and in the pressure of the environment along the segment of thermal protection of length $2L$ can be neglected. Taking into account the conditions of heat insulation at $Y = L$, we can use a one-dimensional approximation in formulation of the boundary-value problem of heat transfer in the insulation layer, which in dimensionless variables has the form

$$C\frac{\partial \theta_i}{\partial \mathrm{Fo}} = \frac{\partial}{\partial X}\left(\Lambda_i \frac{\partial \theta_i}{\partial X}\right); \quad \mathrm{Fo} = 0, \quad X_1 \le X \le X_2: \ \theta = \theta_0, \quad P = P_0, \tag{13}$$

$$X = X_1: \ \theta_i = \theta_{i1} \quad \text{or} \quad \Lambda_i \frac{\partial \theta_i}{\partial X} = H_w \frac{\partial \theta_i}{\partial \mathrm{Fo}}, \tag{14}$$

$$X = X_2: \mathrm{St}_i\,(F - \varepsilon_e \theta_e^4) = H_e \frac{\partial \theta_i}{\partial \mathrm{Fo}} + \Lambda_i \frac{\partial \theta_i}{\partial X}, \tag{15}$$

$$X = \frac{x}{x_3}, \quad \mathrm{Fo} = \frac{t\lambda_i^*}{\rho_i c_i^* x_3^2}, \quad \theta_{i,e} = \frac{T_{i,e}}{T^*}, \quad P = \frac{p}{p^*}, \quad \Lambda_i = \frac{\lambda_i}{\lambda_i^*}, \quad C = \frac{c_i}{c_i^*},$$

$$H_{\text{w,e}} = \frac{(\rho ch)_{\text{w,e}}}{\rho_{\text{i}} c_{\text{i}}^* x_3}, \quad F = \frac{q_{\text{e}}(t)}{\sigma T^{*4}}, \quad \text{St}_{\text{i}} = \frac{\sigma T^{*3} x_3}{\lambda_{\text{i}}^*}, \tag{16}$$

$$\lambda_{\text{i}}^* = \lambda_{\text{i}}(T^*, p^*), \quad c_{\text{i}}^* = c_{\text{i}}(T^*), \quad T^* = 273 \text{ K}, \quad p^* = 10^5 \text{ Pa}.$$

In the approximate external boundary condition (15), we disregard the thermal resistance of the gap between the plate and the external screen and, consequently, the temperature difference between them. The first boundary condition in (14) is used in calculation of combined thermal protection. The condition of continuity of the heat flux, which will be formulated later, serves for determination of an unknown temperature of the reflecting screen θ_{i1}. The second condition in (14) is used for determining the thickness of the plate of radiation thermal protection. In this case, it is assumed that the plate lies directly on the protected structure. The minimum thickness of the plate of the passive system is determined from the condition that during the external thermal effect the temperature of the protected structure does not exceed a specified value $T_{\text{w}}^{\max}$ = 433 K.

Under uniform external conditions, the flow in the vapor-discharge channel is symmetric relative to the line of spreading $y = 0$. The following assumptions relative to the geometric parameters of both systems are introduced:

$$\frac{x_3}{L} << 1, \quad \left(\frac{\delta}{x_1}\right)^2 << 1 \quad \text{or} \quad \left(\frac{\delta}{x_3 - x_2}\right)^2 << 1. \tag{17}$$

Heat and mass transfer in the vapor-discharge channel that satisfies conditions (17) is described by the system of Prandtl equations [12], where the longitudinal pressure gradient is one of the unknown functions. Moreover, these conditions provide a slow flow with a Mach number much smaller than unity [13] and weak evaporation. The latter means that the pressure of the vapor on the evaporation surface can be considered to be equal to the pressure of saturated vapor at the temperature of this surface. Since the pressure of the vapor-air mixture is constant in the cross section of the channel, it satisfies the equation $p = p_{\text{v.s}}(T_{\text{w}}) + (\rho g T)_{\text{w}} R_{\text{a}}$. The formulation of the boundary-value problem considered is stated in [4] in detail.

To calculate the heat and mass transfer in the channel numerically, we supplement (16) with the following dimensionless variables:

$$Y = \frac{y}{L}, \quad \tau = \frac{t u^*}{x_3}, \quad U = \frac{u}{u^*}, \quad V = \frac{v}{Y v^*}, \quad M = \frac{\rho_{\text{v}}}{\rho_{\text{v}}^*}, \quad B = \frac{\partial p}{\partial y} \frac{L}{Y} \frac{1}{\rho_{\text{v}}^* v^{*2}},$$

$$\rho_{\text{v}}^* = \frac{p^*}{R_{\text{v}} T^*}, \quad u^* = \frac{\delta}{L} (R_{\text{v}} T^*)^{1/2}, \quad v^* = u^* \frac{L}{x_3}.$$

The equations of continuity, concentration of the air, y-momentum, state of the vapor-air mixture, energy, and flow rate and total pressure of the mixture with the corresponding boundary conditions in dimensionless form take the following form [4]:

$$\frac{\partial M}{\partial \tau} + MV + \frac{\partial MU}{\partial X} = 0, \quad M \frac{\partial g}{\partial \tau} + MU \frac{\partial g}{\partial X} = \frac{1}{\text{Re}} \frac{\partial}{\partial X} \left(\frac{MD}{\text{Sc}} \frac{\partial g}{\partial X} \right),$$

$$M\frac{\partial V}{\partial \tau}+MV^2+MU\frac{\partial V}{\partial X}+B=\frac{1}{\mathrm{Re}}\frac{\partial}{\partial X}\left(\mu\frac{\partial V}{\partial X}\right),\quad P=M\theta,$$

$$C_p\left(M\frac{\partial \theta}{\partial \tau}+MU\frac{\partial \theta}{\partial X}\right)+\frac{1-\gamma_{\mathrm{v}}}{\gamma_{\mathrm{v}}}\frac{dB}{d\tau}=\frac{1}{\mathrm{Re}}\left[\frac{\partial}{\partial X}\left(\frac{\lambda}{\mathrm{Pr}}\frac{\partial \theta}{\partial X}\right)+\frac{MD}{\mathrm{Sc}}\left(\frac{c_{pa}}{c_{pv}}-1\right)\frac{\partial \theta}{\partial X}\frac{\partial g}{\partial X}\right],$$

$$\int_0^{X_1}\frac{V}{R_{\mathrm{m}}\theta}\,dX=\frac{\Gamma Q}{(\langle R_{\mathrm{m}}\rangle\,\langle\theta\rangle)^{1/2}},\quad \Gamma=\left[\gamma\left(\frac{2}{\gamma-1}\right)^{(\gamma+1)/(\gamma-1)}\right]^{1/2},\tag{18}$$

$$Q(\pi)=1,\quad \pi\equiv\frac{p_{\mathrm{e}}}{p_1}\le\pi_*\equiv\left(\frac{2}{\gamma+1}\right)^{\gamma/(\gamma-1)},\quad Q(\pi)=\left(\frac{\pi}{\pi_*}\right)^{1/\gamma}\left[\frac{\gamma+1}{\gamma-1}\left(1-\pi^{(\gamma-1)/\gamma}\right)\right]^{1/2},\quad \pi>\pi_*,$$

$$P=\frac{1+g_{\mathrm{w}}(R_{\mathrm{a}}-1)}{1-g_{\mathrm{w}}}P_{\mathrm{v.s}}(\theta_{\mathrm{w}});$$

$$\tau=0,\quad 0\le X\le X_1:\ U=V=0,\quad P=P_0,\quad \theta=\theta_0,\quad g=\frac{P_0-P_{\mathrm{v.s}}(\theta_0)}{P_0+(R_{\mathrm{a}}-1)P_{\mathrm{v.s}}(\theta_0)};\tag{19}$$

$$X=0:\ V=0,\quad \frac{D}{\mathrm{Re\,Sc}}\frac{\partial g}{\partial X}=gU;\quad \mathrm{Ko}\,\omega MU+H\frac{\partial \theta}{\partial \tau}=\frac{1}{\mathrm{Re\,Pr}}\left[\lambda\frac{\partial \theta}{\partial X}+\varepsilon_1\,\mathrm{St}\,(\theta_{\mathrm{i1}}^4-\theta^4)\right];\tag{20}$$

$$X=X_1:\ U=V=\frac{\partial g}{\partial X}=0,\quad \theta=\theta_{\mathrm{i1}};\tag{21}$$

$$H(\tau)=\frac{\rho_{\mathrm{w}}c_{\mathrm{w}}h_{\mathrm{w}}}{\rho^*c_{pv}x_3}+\frac{c_{\mathrm{liq}}}{c_{pv}}\left[\frac{m}{\rho^*x_3}-\int_0^{\tau}(MU)_{\mathrm{w}}\,d\tau\right],\tag{22}$$

$$\omega(\theta)=1-\left(\frac{c_{\mathrm{liq}}}{c_{pv}}-1\right)\frac{\theta}{\mathrm{Ko}},\quad R_{\mathrm{m}}(g)=1+g\left(\frac{R_{\mathrm{a}}}{R_{\mathrm{v}}}-1\right),\quad C_p(g)=1+g\left(\frac{c_{pa}}{c_{pv}}-1\right),$$

$$\mathrm{Re}=\frac{\rho^*u^*x_3}{\mu_0},\quad \mathrm{Pr}=\frac{c_{pv}\mu_0}{\lambda_0},\quad \mathrm{Sc}=\frac{\mu_0}{\rho^*D_0},\quad \mathrm{Ko}=\frac{r_0}{c_{pv}T^*},\quad \mathrm{St}=\frac{\sigma T^{*3}x_3}{\lambda_0},\quad \varepsilon_1=\frac{\varepsilon_{\mathrm{w}}\varepsilon_{\mathrm{s}}}{\varepsilon_{\mathrm{w}}+\varepsilon_{\mathrm{s}}-\varepsilon_{\mathrm{w}}\varepsilon_{\mathrm{s}}}.\tag{23}$$

In this problem it is assumed that the coolant is water and the initial temperature of the system is $\theta_0>1$, i.e., the coolant is in the liquid state. Therefore, the density of saturated vapor is described by the empirical formula (10). In Eq. (18), the expression for adiabatic outflow of the gas from the cavity is used. Here $\langle R_{\mathrm{m}}\rangle = R_{\mathrm{m}}(\langle g\rangle)$ and $\langle g\rangle$ and $\langle\theta\rangle$ are the concentration of the air and the temperature averaged across the channel.

The second condition in (20) is the condition of impermeability of the evaporation surface to air. The finite values of the heat capacities of the structure and the coolant and the change in the mass of the latter are allowed for by the presence of the function *H*, which is determined by Eq. (22), where *m* is the initial

TABLE 1. Overall-Dimension-Weight Characteristics of Radiation Thermal Protection and CTP2 (h_i, thickness of the heat insulation, mm; m, mass, kg/m^2)

$h_{i,r.t.p}$	$m_{r.t.p}$	$h_{i,c.t.p}$	m_{liq}	$m_{c.t.p}$	$m_{r.t.p.}/m_{c.t.p}$
95.4	13.4	10	3.93	5.33	2.51
		15	2.93	5.03	2.66
		20	2.29	5.09	2.64

mass of the coolant per unit surface, in the last boundary condition of (20). Here, the radiation heat exchange between the reflecting screen and the evaporation surface, which are considered to be diffusely gray, is also taken into account.

The similarity numbers (23) of the problem depend on the coefficients of viscosity, thermal conductivity, and diffusion of the vapor-air mixture which are calculated with the initial conditions (19). These coefficients of transfer which enter into the equations and boundary conditions are made dimensionless using their initial values. The coefficient of diffusion of the mixture is calculated from the formula $D(T) = 2.16\cdot10^{-5}T^{1.8}$ m^2/sec, the coefficient of viscosity is determined from the Wilkey formula, and the coefficient of thermal conductivity is calculated from the Lehmann formula [14]. The coefficients of transfer of the mixture components are determined from formula (2) for the air, while for the steam they are determined from formulas obtained by numerical interpolation of tabulated data from [15]: $\lambda_v(T = (-5.8 + 0.0856T)\cdot10^{-3}$ W/(m·K), and $\mu_v(T) = (-3.05 + 0.0406T)\cdot10^{-6}$ kg/(m·sec).

The condition of continuity of the heat flux on the screen surface, which serves for determination of its temperature, has the form

$$\frac{\lambda_i}{\lambda_0}\Lambda_i\frac{\partial\theta_i}{\partial X}(X_1, \mathrm{Fo}) = \lambda\frac{\partial\theta}{\partial X}(X_1, \tau) + \varepsilon_1\,\mathrm{St}\,[\theta(X_1, \tau)^4 - \theta(0, \tau)^4]\,.$$

Based on the formulated conjugate boundary-value problem we can calculate the characteristics of CTP2 with the specified changes in the external heat flux and pressure. To compare CTP2 to the passive plate system, we made calculations in which the time dependences $q_e(t)$ and $p_e(t)$ were specified in the form of trapezoids by schematic modeling of the takeoff of an aircraft for 10 min, a cruising flight of 40 min, and landing for 10 min. In the calculations, the external heat flux changed from 0 to a maximum value of 10^5 W/m^2 and again to 0; the pressure of the environment changed from the initial value $p_0 = 10^5$ Pa to a minimum value of 500 Pa and then increased to the initial value. The initial temperature of both the passive and combined systems was $T_0 = 290$ K.

The parameters of the quartz plate used as a high-temperature heat insulation have been determined above. All the parameters of CTP2, except for the plate thickness, were specified: $L = 0.5$ m, $x_1 = 0.01$ m, $\delta = 5\cdot10^{-5}$ m, $\varepsilon_0 = 0.1$, and $\varepsilon_w = \varepsilon_e = 0.8$. It is assumed that the protected structure is made of aluminum alloy and has the following parameters: $h_w = 0.002$, $\rho_w = 2800$ kg/m^3, and $c_w = 900$ J/(kg·K).

The dependence of the total weight of CTP2 $m_{c.t.p} = \rho_i h_i + m$ on the thickness of heat insulation is of principal interest. The initial mass of the coolant m was determined by iteration from the condition that by the end of the thermal effect the coolant is evaporated completely. The results of comparative calculations of radiation and combined systems are presented in Table 1, where the values of the plate thickness are given in mm and those of mass are given in kg/m^2.

It can be noted that the thickness of the plate in the passive system is virtually unacceptable for the considered mode of external thermal effect. The combined system of thermal protection can guarantee not only the real thickness of the thermal protection but also a considerable decrease in the total weight of it.

Modeling of CTP3. This version of the system of thermal protection combines the properties of radiation, evaporation, and transpiration systems. In what follows, we consider the three main parts of CTP3: an evaporation cavity (region 1), a layer of porous insulation (region 2), and a vapor-discharge channel (region 3). The corresponding subscripts are used to denote the pressure in these three regions.

The boundary-value problem is formulated in a one-dimensional approximation with the following additional simplifications. Since the heat capacity of the vapor per unit volume is much lower than that in the porous insulation, we can neglect the nonstationary term in the equation of energy for the vapor. It is also assumed that the hydrodynamic time of relaxation of the flow $t_u = x_3/u^*$ is small compared to the characteristic time of warming-up of the system under the action of the external thermal effect. Under these assumptions, vapor transfer can be considered in a quasistationary approximation, i.e., time as a parameter enters into all the equations describing vapor flow. The presence of the air in CTP3 is disregarded in this formulation of the problem.

It follows from the equations of continuity and momentum that across the evaporation cavity both the vapor flow and the pressure are constant, with the latter being equal to the pressure of saturated vapor at the temperature of the evaporation surface. In the equation of energy, convective and conductive terms are taken into account. The boundary condition on the evaporation surface reflects the fact that heating of the protected structure and evaporation of the coolant occur due to conductive-convective heat transfer in the gas phase and radiative heat exchange between the surfaces of the coolant carrier and the porous heat insulation.

Thus, the equations of heat and mass transfer with the corresponding boundary conditions in the evaporation cavity have the following form:

$$\rho_{\rm v} u = j\,(t)\,, \quad p_1 = p_{\rm v.s}\,(T_{\rm w})\,, \quad jc_{p\rm v}\frac{dT_{\rm v}}{dx} = \frac{d}{dx}\left(\lambda_{\rm v}\frac{dT_{\rm v}}{dx}\right),$$

$$x = 0:\ \rho_{\rm w} c_{\rm w} h_{\rm w}\frac{dT_{\rm w}}{dt} + rj = \lambda_{\rm v}\frac{dT_{\rm v}}{dx} + \varepsilon_1\sigma\,(T_{\rm i1}^4 - T_{\rm w}^4)\,, \quad r = r_0 - (c_{\rm liq} - c_{p\rm v})\,T\,.$$

Heat and mass transfer in a porous layer of heat insulation is modeled with allowance for the temperature difference between the vapor and the porous medium and with allowance for the interphase heat transfer. Vapor flow in the porous insulation is assumed to be slow; therefore, it is described by the Darcy equation

$$j = -\frac{K}{\mu_{\rm v}}\rho_{\rm v}\frac{dp_2}{dx}\,. \tag{24}$$

The continuity equation for region 2 yields $j = j(t)$. Taking account of this fact and of the equation of state of an ideal gas, we can integrate (24) and obtain the formula for the vapor pressure in the porous layer:

$$p_2\,(x,\,t) = \left(p_1^2 - 2j\frac{R_{\rm v}}{K}\int\limits_{x_1}^{x}\mu_{\rm v}T_{\rm v}dx\right)^{1/2}.$$

We give the equation of energy of the vapor with account for the interphase heat transfer in the porous layer:

$$jc_{p\rm v}\frac{dT}{dx} + s\kappa\,(T_{\rm v} - T_{\rm i}) = \frac{d}{dx}\left(\lambda_{\rm v}\frac{dT_{\rm v}}{dx}\right). \tag{25}$$

Here s and κ are the effective area of the inner surface of the porous body per unit of its volume and the coefficient of convective heat transfer.

The equation of energy of the porous layer and the corresponding boundary conditions have the following form:

$$\rho_i c_i \frac{\partial T_i}{\partial t} + s\kappa (T_i - T_v) = \frac{\partial}{\partial x}\left(\lambda_i \frac{\partial T_i}{\partial x}\right);$$

$$x = x_1 : \ \lambda_i \frac{\partial T_i}{\partial x} = \varepsilon_1 \sigma (T_i^4 - T_w^4) , \tag{26}$$

$$x = x_2 : \ \lambda_i \frac{\partial T_i}{\partial x} = \varepsilon_2 \sigma (T_e^4 - T_i^4) , \quad \varepsilon_2 = \frac{\varepsilon_i \varepsilon_e}{\varepsilon_i + \varepsilon_e - \varepsilon_i \varepsilon_e} .$$

In order to simplify this consideration we assume that all quartz fibers, which form the plate, have the shape of round cylinders of the same diameter d and are perpendicular to the x axis. In this case, the specific internal area of the porous body is estimated as $s = 4(1 - \Pi)/d$.

Convective heat exchange between the gas and the porous matrix is a complex process. The relation between local Nusselt ($\mathrm{Nu} = \kappa d/\lambda_v$) and Reynolds ($\mathrm{Re} = \rho_v u d/\mu_v$) numbers is usually used for determination of the coefficient of convective heat transfer in porous bodies [16]. In the present work, the correlation equation for a single cylinder from [17]

$$\mathrm{Nu} = (0.4\ \mathrm{Re}^{1/2} + 0.06\ \mathrm{Re}^{2/3})\ \mathrm{Pr}^{2/5} \left[\frac{\mu_v (T_v)}{\mu_v (T_i)}\right]^{1/4} .$$

is taken for estimation of the effective coefficient of heat transfer.

We note that the boundary conditions for Eq. (26) take into account only the radiative heat exchange between the surfaces of the insulation, the coolant carrier, and the external screen, since conductive and convective heat transfer in regions 1 and 3 is provided by the gas phase. In our consideration, the effective coefficient of thermal conductivity of the insulation is determined by Eq. (1), where only the first two terms, i.e., the thermal conductivity of a solid matrix and radiation, are taken into account. Convective heat transfer in region 2 is described by Eq. (25).

As has been noted in the previous section, the component of the longitudinal velocity and the pressure gradient in a flat channel with converging ends can be represented in the form $v = yw(t)$ and $\partial p_3/\partial y = yE(t)$. Then, in the quasistationary approximation, the equations of energy, continuity, and momentum, which describe vapor flow in region 3, have the form

$$\rho_v u c_{pv} \frac{dT_v}{dx} = \frac{d}{dx}\left(\lambda_v \frac{dT_v}{dx}\right); \quad x = x_3 : \ T_v = T_e ;$$

$$\rho_v u = j - \int_{x_2}^{x} \rho_v w dx ; \ x = x_3 : \ u = 0 ; \tag{27}$$

$$\rho_v u \frac{dw}{dx} + \rho_v w^2 + E = \frac{d}{dx}\left(\mu_v \frac{dw}{dx}\right); \quad x = x_2, x_3 : \quad w = 0 .$$

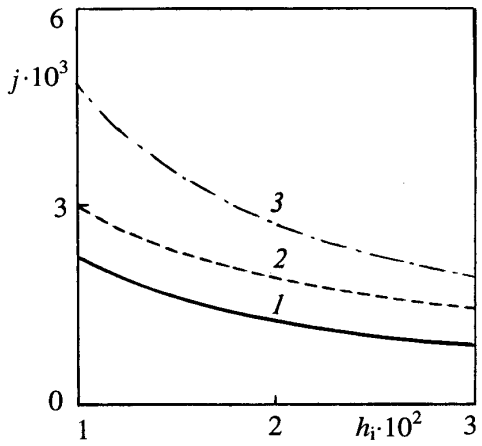

Fig. 2. Dependences of the rate of evaporation of the coolant on the thickness of the heat insulation. j, kg/(m·sec); h_i, m.

By analogy with the previous section, the unknown second derivative of pressure along the channel E is determined from the condition of non-flow on the surface of the external screen. Moreover, the rate of evaporation which enters into (27) is related to the vapor flow rate through the drainage hole:

$$\Gamma \delta p_3 (R_v \langle T_v \rangle)^{-1/2} Q(\pi) = jL ,$$

where Γ and $Q(\pi)$ are determined by Eqs. (18).

The initial temperature of the system and the gas pressure in it are specified:

$$t = 0 : \; T_i = T_v = T_0 , \;\; p = p_0 .$$

If the condition $p_0 > p_{v.s}(T_0)$ is satisfied, then in calculations it is assumed that, as long as $p_e > p_{v.s}(T_w)$ at the nonstationary stage of heating, the pressure in all parts of the thermal-protection system is equal to the external pressure and the rate of evaporation of the coolant can be neglected [4]. When the condition $p_{v.s}(T_w) \geq p_e(t)$ is reached, the formulated boundary-value problem is solved without additional simplifications.

On the basis of the model suggested, we calculated heat and mass transfer in CTP3 for the same specified parameters as in the case of calculation of CTP2. We specified the additional parameters which are substantial for analysis of CTP3, namely: the width of the external channel $x_3 - x_2 = 0.001$ m, the radiating powers of all the surfaces participating in radiative heat transfer $\varepsilon_{e,i,w} = 0.8$, the porosity of the heat insulation $\Pi = 0.9$, its permeability $K = 10^{-12}$ m^2, and the diameter of fibers $d = 2 \cdot 10^{-4}$ m. The initial values of the temperature and the pressure were $T_0 = 300$ K and $p_0 = 10^5$ Pa. The temperature of the external screen and the pressure of the environment were found in the form of linear functions of time which change to their limiting values $T_e^{max} = 1500$ K and $p_e^{min} = 500$ Pa. Then, both the temperature of the screen and the external pressure remained constant.

The effect of the thickness of the heat insulation on the steady rate of evaporation of the coolant is shown in Fig. 2; it is seen that curve 1 corresponds to CTP3, curve 2 represents the results for CTP2 where the radiating power of the internal reflecting screen is $\varepsilon_s = 0.1$, and curve 3 corresponds to CTP2 and the radiating power of the screen augmented to $\varepsilon_s = 0.8$.

The advantage of CTP3 (see Fig. 2) is related to the employment, to a certain degree, of the principle of a transpiration system. In this case, heating of the vapor to the temperature of the external screen allows one to use its heat capacity along with the heat of evaporation. Figure 2 demonstrates the considerable effect of the radiating power of the reflecting screen in CTP2. It is of interest that the ratio of the rates of evapo-

ration j_3/j_2 (CTP3/CTP2) is constant and equals 0.46 within the considered range of variation of the plate thickness for the high radiating power of the reflecting screen $\varepsilon_s = 0.8$ in CTP2. When $\varepsilon_s = 0.1$, the indicated ratio decreases with increase in the insulation thickness: $j_3/j_2 = 0.75$, 0.66, and 0.61 for $h_i = 1$, 2, and 3 cm, respectively, i.e., the efficiency of CTP3 increases compared to the efficiency of CTP2. Since the minimum total weight of the radiation-evaporation thermal protection is reached with approximately equal masses of the heat insulation and the initial supply of the coolant [3, 4], the ratio of the minimum weights of CTP2 and CTP3 can be estimated by the ratio of evaporation rates of the coolant.

Conclusions. Theoretical and experimental investigations show that there is a possibility of simultaneously decreasing the thickness of the layer of heat insulation (2–6 times) and the total weight of the combined systems of thermal protection (to 3 times) compared to their values in the passive plate thermal protection. The suggested mathematical models of combined systems allow calculation of the main characteristics of them, in particular, the rate of evaporation of the coolant and the distributions of temperature and pressure. It is shown that the combined system, in which the coolant vapor flows through the layer of porous insulation, is the most efficient among those considered.

NOTATION

a, coefficient of transfer of the liquid; *b*, mean diameter of the pores; *B*, dimensionless second derivative of pressure; *c*, specific heat capacity; *C*, dimensionless specific heat capacity; *d*, mean diameter of the fibers; *D*, coefficient of diffusion; *E*, second derivative of pressure; *f*, function of the transient state; *F*, dimensionless heat flux; *g*, concentration of air; *G*, gas flow rate through the hole; *h*, thickness; *H*, dimensionless total heat capacity; *j*, mass flow; *K*, permeability; *l*, mean free path of molecules; *L*, half-length of the fragment of thermal protection; *M*, dimensionless density of the vapor; *p*, pressure; *P*, dimensionless pressure; *q*, heat flux; *Q*, dimensionless function of the flow rate; *r*, specific heat of evaporation; *R*, gas constant; *S*, area of the model base; *t*, time; *T*, temperature; *u* and *v*, velocity components; *U* and *V*, dimensionless velocity components; *W*, internal volume of the model; *x*, *y*, coordinates; *X*, *Y*, dimensionless coordinates; *Z*, ratio of the densities; α, moisture content; β, heat-transfer coefficient; δ, width of the drainage slot; ε, radiating power; γ, adiabatic index; λ, coefficient of thermal conductivity; Λ, dimensionless coefficient of thermal conductivity; μ, coefficient of dynamic viscosity; π, ratio of the pressures; Π, porosity; ρ, density; σ, Stefan–Boltzmann constant; τ, dimensionless time; ω, dimensionless heat of evaporation; ξ, coefficient of accommodation; Fo, Fourier number; Ko, Kossovich number; Nu, Nusselt number; Pr, Prandtl number; Re, Reynolds number; Sc, Schmidt number; St, Stark number. Super- and subscripts: 0, initial values; a, air; c, cover of the model; c.c, coolant carrier; c.t.p, combined thermal protection; d, damping layer; e, external conditions and parameters; eff, effective value; f, base (foundation) of the model; g, gas; i, heat insulation; liq, liquid; leak, displaced; m, vapor-air mixture; *p*, at constant pressure; r, radiation; r.t.p, radiation thermal protection; s, reflecting screen; v, vapor; *v*, at constant volume; v.s, saturated vapor; w, wall; *, characteristic quantities.

REFERENCES

1. L. Roberts, *Adv. Aeronaut. Sci.* (New York), **4**, 1019–1044 (1962).
2. I. N. Bobrov and A. P. Kuryachii, *Teplofiz. Vys. Temp.*, **34**, No. 1, 75–82 (1996).
3. J. H. Bridges and E. D. Richmond, *Techn. Lunar Explorat.* (New York–London), 761–782 (1963).
4. A. P. Kuryachii, *Izv. Ross. Akad. Nauk, Mekh. Zhidk. Gaza*, No. 1, 24–36 (1995).
5. V. N. Anan'ev and A. P. Kuryachii, *Teplofiz. Vys. Temp.*, **30**, No. 6, 1194–1202 (1992).
6. W.-D. Ebeling, W. P. P. Fisher, J. Antonenko, and L. Paderin, *SAE Tech. Paper Series* No. 951577, 1–9 (1995).

7. S. Whitaker, *Adv. Heat Transfer* (New York), **13**, 540–547 (1977).
8. S. B. Nasrallah and P. Perre, *Int. J. Heat Mass Transfer*, **31**, No. 5, 957–967 (1988).
9. I. N. Bobrov and A. P. Kuryachii, *Teplofiz. Vys. Temp.*, **32**, No. 3, 441–445 (1994).
10. A. V. Luikov, *Heat and Mass Transfer, Handbook* [in Russian], Moscow (1978).
11. G. N. Abramovich, *Applied Gas Dynamics* [in Russian], Moscow (1969).
12. J. C. Williams, *AIAA J.*, **1**, No. 1, 185–195 (1963).
13. H. Van Ooijen and C. J. Hoogendoorn, *AIAA J.*, **17**, No. 11, 1251–1259 (1979).
14. S. Bretsznajder, *Wlasnosci Gazow i Cieszy* [in Polish], Warsaw (1962).
15. M. P. Vukalovich, *Thermophysical Properties of Water and Steam* [in Russian], Moscow (1967).
16. S. Maruyama and R. Viskanta, *AIAA Pap.* No. 605, 1–11 (1989).
17. S. Whitaker, *AIChE J.*, **18**, No. 2, 361–370 (1972).